



R. Barretta · S. Ali Faghidian · F. Marotti de Sciarra

# Aifantis versus Lam strain gradient models of Bishop elastic rods

Received: 9 March 2019 / Published online: 18 May 2019  
© Springer-Verlag GmbH Austria, part of Springer Nature 2019

**Abstract** In this paper, the size-dependent static behavior of Bishop rods is investigated by Lam and Aifantis strain gradient formulations of elasticity. Appropriate constitutive boundary conditions are established for both the theories by making recourse to a variational approach. Unlike contributions of literature, no higher-order kinematic and static boundary conditions, which have not a clear physical meaning, are required to close the relevant gradient problems. The proposed methodology leads to mathematically well-posed elastostatic problems and is illustrated by examining size effects in selected thick rods of nanotechnological interest. Exact solutions of Bishop nano-rods are detected for a variety of loading systems and kinematic boundary conditions. Peculiar properties, merits, and implications of both the strain gradient formulations, equipped with the proper boundary conditions, are illustrated and commented. The outcomes can be useful for the design and optimization of rod-like thick components of nanoelectromechanical systems.

## 1 Introduction

The examination of the mechanical response of nano-structures is the major focus of recent researches in the literature as a result of extensive exploitations of nano-structured elements in the fabrication of nanoelectromechanical systems (NEMS). Local continuum mechanics is not able to investigate the structural behavior of nano-devices [1, 2]. Adoption of nonlocal formulations is therefore indispensable to capture size effects [3–7]. Modeling of small-scale phenomena in nano-structures is a topic of current interest in the scientific community [8–36]. Recent reviews on the matter are tackled in [37–39].

In the nonlocal theory of elasticity, the output field at a point of a continuum is assumed to be the integral convolution between the elastic source field and a suitable averaging kernel. Nowadays, based on adopting strain- or stress-driven formulations, two different nonlocal elasticity models are available. While Eringen's strain-driven law is well established to lead to ill-posed nano-engineering problems which are defined in bounded domains [40–42], the stress-driven nonlocal model provides a well-posed and efficient approach to appropriately assess size effects in a wide range of structural problems of technical interest [43–58].

Mindlin in his milestone work [59] introduced the strain gradient theory of elasticity (SGT), where the material response at a point of a continuum is dependent on both the strain and the strain gradients of different

---

R. Barretta (✉) · F. Marotti de Sciarra  
Department of Structures for Engineering and Architecture, University of Naples Federico II, via Claudio 21, 80125 Naples, Italy  
E-mail: rabarret@unina.it

F. Marotti de Sciarra  
E-mail: marotti@unina.it

S. A. Faghidian  
Department of Mechanical Engineering, Science and Research Branch, Islamic Azad University, Tehran, Iran  
E-mail: faghidian@gmail.com

orders. Application of the Mindlin model is intricate in the primary mathematical framework, and therefore, a range of reduced strain gradient models were introduced and discussed in literature [60–67]. The strain gradient theory of Mindlin [59] includes five extra characteristic length-scale parameters being difficult to be determined theoretically and experimentally. A simplified strain gradient theory of elasticity was then presented by Aifantis [60] with only one characteristic length-scale parameter.

Aifantis strain gradient theory, including Laplacian-type gradients, is more convenient to be employed from physical and mathematical points of view. The modified strain gradient elasticity theory was established by Lam et al. [61] wherein an appropriate equilibrium equation governing higher-order stresses was added to the classical equilibrium conditions. The number of length-scale parameters in Lam strain gradient model is reduced to three, characterizing dilatation gradient, deviatoric stretch gradient, and symmetric rotation gradient. Both modified and simplified strain gradient models of elasticity have been widely applied by the scientific community to capture size-dependent responses of micro- and nano-structures. The size-dependent formulations founded on the modified and simplified SGTs lead to well-posed problems provided that suitable constitutive boundary conditions are prescribed.

## 2 Motivation and outline

The simple rod model is well known to be appropriate merely for slender structures, and thus, lateral deformation and shear stiffness effects have to be accounted for stubby rods [68,69]. A variety of nonlocal theories have been employed to analyze the size-dependent structural response of thick nano-rods including Eringen differential nonlocal model [70–77], strain gradient elasticity theory [78], modified couple stress theory [79,80], and unified gradient theory of elasticity [81–85]. Almost all of the presented results in literature, based on the gradient theories of elasticity, are dedicated to investigate the propagation of longitudinal stress waves in unbounded domains [78–85], and consequently, the issue of constitutive boundary conditions is omitted. According to Güven [78], “for a finite bar, such a model has to be completed with higher-order boundary conditions that can be obtained from the application of variational principles”. Furthermore, in few cases where the higher-order boundary conditions are introduced for a finite Bishop nano-rod [81,83], the number of the prescribed boundary conditions exceeds the order of differential conditions of equilibrium.

Therefore, the contributions presented in the literature on examination of Bishop nano-rods in the framework of both the modified and simplified strain gradient elasticity theories should be amended to properly take the constitutive boundary conditions into account.

The motivation of the present research is in equipping the Aifantis and Lam strain gradient formulations of Bishop elastic nano-rods with appropriate constitutive boundary conditions. The corresponding elastostatic problems of Bishop rods are well posed, so that an effective strategy is provided to assess small-size effects in stubby nano-rods. The plan is as follows. Differential and boundary conditions of equilibrium of Bishop local rods are briefly evoked in Sect. 2. Aifantis and Lam strain gradient elasticity theories for Bishop rods are developed in Sect. 3, and the suitable constitutive boundary conditions are established for every model. The gradient models in Sect. 3 are then adopted in Sect. 4 to establish exact solutions of Bishop rods for selected loadings and kinematic boundary conditions of engineering interest. New numerical benchmarks are detected for gradient stubby nano-rods.

## 3 Bishop local rod

A homogenous elastic thick rod with length  $L$ , area  $A$ , and cross section  $\Xi$ , subjected to a distributed axial force per unit length  $p$  and concentrated forces  $\bar{N}$  at the rod ends is examined here. Axial, radial, and circumferential coordinates describing the position of the rod points with respect to the cross section centroid are, respectively, designated by  $x$ ,  $r$ , and  $\theta$ . The investigated formulation of the elastic thick rod is considered to be axisymmetric, and therefore, the circumferential displacement  $u_\theta$  can be omitted. Vanishing of the radial stress on the cross section leads to the subsequent displacement field of a Bishop thick rod [86]

$$u_x(x, r) = u(x), \quad u_r(x, r) = -vr\partial_x u(x), \quad u_\theta(x, r) = 0, \quad (1)$$

with  $\nu$  Poisson’s ratio.  $u_x$ ,  $u_r$ , and  $u_\theta$  correspondingly representing axial, radial, and circumferential displacement components. The displacement field as Eq. (1) noticeably includes the lateral deformation effects. The nonvanishing dual fields of strains and stresses in the thick rod elastic model are given by

$$\varepsilon_x = \partial_x u, \quad \gamma_{xr} = -\nu r \partial_x^2 u, \tag{2.1,2}$$

$$\sigma_x = E \varepsilon_x = E \partial_x u, \quad \tau_{xr} = G \gamma_{xr} = -G \nu r \partial_x^2 u \tag{2.3,4}$$

where  $\varepsilon_x$ ,  $\sigma_x$  and  $\gamma_{xr}$ ,  $\tau_{xr}$  correspondingly designate axial and shear strain and stress fields. Shear and Euler-Young moduli are also denoted by  $G$  and  $E$ , where  $G = E/2(1 + \nu)$ .

The Bishop rod local elastic model is formulated by assuming that the elastic energy depends on the axial strain field  $\varepsilon \in C^2([0, L]; \mathfrak{R})$  as

$$\Pi(\varepsilon) := \frac{1}{2} \int_0^L \left( \int_{\Xi} (E \varepsilon_x^2 + G \gamma_{xr}^2) dA \right) dx = \frac{1}{2} \int_0^L EA \left( \varepsilon_x^2 + \frac{\nu^2 \rho^2}{2(1 + \nu)} (\partial_x \varepsilon_x)^2 \right) dx \tag{3}$$

where the gyration radius is defined as  $\rho := \sqrt{J/A}$  with  $J$  being the polar moment of inertia about the center of the cross section.

The corresponding stress field in an elastic thick rod is the axial force field  $N \in C^1([0, L]; \mathfrak{R})$  which can be determined by the variational constitutive condition for any virtual axial strain field  $\delta\varepsilon \in C^1([0, L]; \mathfrak{R})$

$$\langle N, \delta\varepsilon \rangle := \int_0^L N(x) \delta\varepsilon(x) dx = \langle d\Pi(\varepsilon), \delta\varepsilon \rangle. \tag{4}$$

In view of the elastic energy  $\Pi$  as Eq. (3), the derivative of the elastic energy along a virtual axial strain field can be directly evaluated as

$$\langle d\Pi(\varepsilon), \delta\varepsilon \rangle = \int_0^L EA \varepsilon_x \delta\varepsilon_x dx + \int_0^L EA \frac{\nu^2 \rho^2}{2(1 + \nu)} (\partial_x \varepsilon_x) \partial_x (\delta\varepsilon_x) dx. \tag{5}$$

Integrating by parts Eq. (5) while imposing the variational condition Eq. (4), a standard localization procedure provides the following differential problem equipped with constitutive boundary conditions:

$$\begin{cases} EA \left( \varepsilon - \frac{\nu^2 \rho^2}{2(1 + \nu)} \partial_x^2 \varepsilon \right) = N, & \text{in } [0, L] \\ \nu^2 \rho^2 \partial_x \varepsilon_x = 0, & \text{on } \partial [0, L] \end{cases} \tag{6}$$

with  $\partial [0, L]$  denoting the boundary of the interval  $[0, L]$ . The classical elastic law of slender rods is recovered as the Poisson ratio  $\nu$  vanishes in Eq. (6).

The differential and boundary conditions of static equilibrium of rods are also recalled as

$$\partial_x N + p = 0, \tag{7.1}$$

$$(N + \bar{N}) \delta u|_{x=0} = (N - \bar{N}) \delta u|_{x=L} = 0. \tag{7.2}$$

It can be noticeably deduced from the established boundary-value problem that the Bishop elastic rod model contains both the lateral deformation and shear stiffness effects.

### 4 Strain gradient Bishop rod models

#### 4.1 Lam strain gradient model

The strain energy of a Bishop elastic rod in the framework of Lam SGT can be detected in terms of the axial strain field  $\varepsilon \in C^2([0, L]; \mathfrak{R})$  as [78]

$$\begin{aligned} \Pi_{\text{Lam}}^{\text{SGT}}(\varepsilon) = & \frac{1}{2} \int_0^L EA \left( \varepsilon_x^2 + \left( \frac{\nu^2 \rho^2}{2(1 + \nu)} + \ell_0^2 \frac{(1 - 2\nu)^2}{(1 + \nu)} + \ell_1^2 \frac{2(1 + 2\nu)^2}{5(1 + \nu)} \right) (\partial_x \varepsilon_x)^2 \right. \\ & \left. + \left( \ell_1^2 \frac{4\nu^2 \rho^2}{15(1 + \nu)} + \ell_2^2 \frac{\nu^2 \rho^2}{8(1 + \nu)} \right) (\partial_x^2 \varepsilon_x)^2 \right) dx \end{aligned} \tag{8}$$

with  $\ell_0$ ,  $\ell_1$ , and  $\ell_2$  being the length-scale parameters associated with dilatation gradients, deviatoric stretch gradients, and symmetric rotation gradients, respectively.

The axial force field  $N \in C^1([0, L]; \mathfrak{R})$  in a Bishop gradient rod is the dual scalar field of any virtual axial strain field  $\delta\varepsilon \in C^1([0, L]; \mathfrak{R})$ , according to the following variational rule:

$$\langle N, \delta\varepsilon \rangle := \int_0^L N(x) \delta\varepsilon(x) dx = \langle d\Pi_{\text{Lam}}^{\text{SGT}}(\varepsilon), \delta\varepsilon \rangle. \quad (9)$$

The right-hand side of Eq. (9) can be determined by evaluating the derivative of the elastic energy  $\Pi_{\text{Lam}}^{\text{SGT}}$  Eq. (8) along a virtual axial strain field  $\delta\varepsilon \in C^1([0, L]; \mathfrak{R})$ ,

$$\begin{aligned} \langle d\Pi_{\text{Lam}}^{\text{SGT}}(\varepsilon), \delta\varepsilon \rangle &= \int_0^L EA \varepsilon_x \delta\varepsilon_x dx \\ &+ \int_0^L EA \left( \frac{v^2 \rho^2}{2(1+\nu)} + \ell_0^2 \frac{(1-2\nu)^2}{(1+\nu)} + \ell_1^2 \frac{2(1+2\nu)^2}{5(1+\nu)} \right) (\partial_x \varepsilon_x) \partial_x (\delta\varepsilon_x) dx \\ &+ \int_0^L \left( \ell_1^2 \frac{4v^2 \rho^2}{15(1+\nu)} + \ell_2^2 \frac{v^2 \rho^2}{8(1+\nu)} \right) (\partial_x^2 \varepsilon_x) \partial_x^2 (\delta\varepsilon_x) dx. \end{aligned} \quad (10)$$

The Lam strain gradient elasticity law of Bishop's rod is then obtained by integrating by parts Eq. (10) and enforcing the variational condition Eq. (9). The associated constitutive differential and boundary conditions are got by resorting to a standard localization procedure,

$$\left\{ \begin{array}{l} N = EA \left( \varepsilon - \left( \frac{v^2 \rho^2}{2(1+\nu)} + \ell_0^2 \frac{(1-2\nu)^2}{(1+\nu)} + \ell_1^2 \frac{2(1+2\nu)^2}{5(1+\nu)} \right) \partial_x^2 \varepsilon + \left( \ell_1^2 \frac{4v^2 \rho^2}{15(1+\nu)} + \ell_2^2 \frac{v^2 \rho^2}{8(1+\nu)} \right) \partial_x^4 \varepsilon \right) \quad \text{in } [0, L], \quad (11.1) \end{array} \right.$$

$$\left\{ \begin{array}{l} \left( \frac{v^2 \rho^2}{2(1+\nu)} + \ell_0^2 \frac{(1-2\nu)^2}{(1+\nu)} + \ell_1^2 \frac{2(1+2\nu)^2}{5(1+\nu)} \right) \partial_x \varepsilon - \left( \ell_1^2 \frac{4v^2 \rho^2}{15(1+\nu)} + \ell_2^2 \frac{v^2 \rho^2}{8(1+\nu)} \right) \partial_x^3 \varepsilon = 0 \quad \text{on } \partial[0, L], \quad (11.2) \end{array} \right.$$

$$\left\{ \begin{array}{l} \left( \ell_1^2 \frac{4v^2 \rho^2}{15(1+\nu)} + \ell_2^2 \frac{v^2 \rho^2}{8(1+\nu)} \right) (\partial_x^2 \varepsilon_x) = 0 \quad \text{on } \partial[0, L]. \quad (11.3) \end{array} \right.$$

#### 4.2 Aifantis strain gradient model

The gradient model of a Bishop elastic rod according to Aifantis SGT can be also formulated by assuming that the elastic energy depends on the axial strain field  $\varepsilon \in C^2([0, L]; \mathfrak{R})$  as

$$\begin{aligned} \Pi_{\text{Aifantis}}^{\text{SGT}}(\varepsilon) &:= \frac{1}{2} \int_0^L \left( \int_{\Xi} (E \varepsilon_x^2 + G \gamma_{xr}^2) dA \right) dx + \frac{1}{2} \ell_s^2 \int_0^L \left( \int_{\Xi} (E (\partial_x \varepsilon_x)^2 + G (\partial_x \gamma_{xr})^2) dA \right) dx \quad (12) \\ &= \frac{1}{2} \int_0^L EA \left( \varepsilon_x^2 + \left( \frac{v^2 \rho^2}{2(1+\nu)} + \ell_s^2 \right) (\partial_x \varepsilon_x)^2 + \ell_s^2 \frac{v^2 \rho^2}{2(1+\nu)} (\partial_x^2 \varepsilon_x)^2 \right) dx \end{aligned}$$

where in accordance with Aifantis SGT, the gradient characteristic length  $\ell_s$  is introduced to establish the significance of the first-order strain gradient field.

In consequence of application of the similar standard variational procedure, as earlier employed for the Lam SGT, the constitutive differential and boundary conditions of Bishop elastic rods in the framework of Aifantis SGT are determined as

$$\left\{ \begin{array}{l} N = EA \left( \varepsilon - \left( \frac{v^2 \rho^2}{2(1+\nu)} + \ell_s^2 \right) \partial_x^2 \varepsilon + \ell_s^2 \frac{v^2 \rho^2}{2(1+\nu)} \partial_x^4 \varepsilon \right) \quad \text{in } [0, L], \quad (13.1) \end{array} \right.$$

$$\left\{ \begin{array}{l} \left( \frac{v^2 \rho^2}{2(1+\nu)} + \ell_s^2 \right) \partial_x \varepsilon - \ell_s^2 \frac{v^2 \rho^2}{2(1+\nu)} \partial_x^3 \varepsilon = 0 \quad \text{on } \partial[0, L], \quad (13.2) \end{array} \right.$$

$$\left\{ \begin{array}{l} \ell_s^2 \frac{v^2 \rho^2}{2(1+\nu)} \partial_x^2 \varepsilon = 0 \quad \text{on } \partial[0, L]. \quad (13.3) \end{array} \right.$$

Noticeably, both the modified and simplified strain gradient laws of a Bishop elastic rod have similar mathematical form, though with different strain gradient coefficients in prescription of the constitutive differential and boundary conditions.

## 5 Exact analytical solutions and illustrations

Aifantis and Lam strain gradient elasticity theories are exploited here to analyze the elastostatic behavior of Bishop nano-rods subjected to a variety of loading systems and kinematic boundary conditions. To suitably compare the size-dependent response of Bishop nano-rods consistent with the modified and simplified strain gradient models, the effects corresponding to each gradient parameter in the Lam SGT are first examined independently. Afterward to analyze the size-dependent axial displacement of Bishop nano-rods, the length-scale parameters  $\ell_0$ ,  $\ell_1$ , and  $\ell_2$  of Lam SGT, characterizing dilatation, stretch, and rotation gradient, are assumed to be equal,  $\ell_0 = \ell_1 = \ell_2$ .

The non-dimensional parameters: axial abscissa  $\bar{x}$ , characteristic parameter  $\lambda$ , axial displacement  $\bar{u}$  as well as the radius of gyration  $\bar{\rho}$  are defined, for a nano-rod subjected to uniform axial load intensity  $\bar{p}$ , by

$$\bar{x} = \frac{x}{L}, \quad \lambda = \frac{\ell}{L}, \quad \bar{u}(\bar{x}) = u(x) \frac{EA}{\bar{p}L^2}, \quad \bar{\rho} = \frac{\rho}{L}. \quad (14)$$

For a nano-rod subjected to a concentrated tensile tip-load  $\bar{N}$ , the non-dimensional axial displacement  $\bar{u}$  is introduced as

$$\bar{u}(\bar{x}) = u(x) \frac{EA}{\bar{N}L}. \quad (15)$$

To examine the elastostatic behavior of Bishop strain gradient nano-rods, the differential condition of equilibrium Eq. (7.1) should be first integrated. The axial force field can be accordingly obtained in terms of an integration constant  $\Lambda_1$  as

$$N(x) = - \int_0^x p(\zeta) d\zeta + \Lambda_1. \quad (16)$$

The axial strain field  $\varepsilon$  may be afterward determined by solving the constitutive differential equation of Lam SGT Eq. (11.1) or Aifantis SGT Eq. (13.1) in terms of the integration constants  $\{\Lambda_2, \Lambda_3, \Lambda_4, \Lambda_5\}$  as

$$\begin{aligned} \varepsilon(x) = & \Lambda_2 \exp(-\alpha_1 x) + \Lambda_3 \exp(\alpha_1 x) + \Lambda_4 \exp(-\alpha_2 x) + \Lambda_5 \exp(\alpha_2 x) \\ & + \exp(\alpha_1 x) \int_0^x \exp(-\alpha_1 \xi_1) \frac{N(\xi_1) \alpha_1 \alpha_2^2}{EA(2\alpha_1^2 - 2\alpha_2^2)} d\xi_1 - \exp(-\alpha_1 x) \int_0^x \exp(\alpha_1 \xi_2) \frac{N(\xi_2) \alpha_1 \alpha_2^2}{EA(2\alpha_1^2 - 2\alpha_2^2)} d\xi_2 \\ & + \exp(-\alpha_2 x) \int_0^x \exp(\alpha_2 \eta_1) \frac{N(\eta_1) \alpha_1^2 \alpha_2}{EA(2\alpha_1^2 - 2\alpha_2^2)} d\eta_1 - \exp(\alpha_2 x) \int_0^x \exp(-\alpha_2 \eta_2) \frac{N(\eta_2) \alpha_1^2 \alpha_2}{EA(2\alpha_1^2 - 2\alpha_2^2)} d\eta_2 \end{aligned} \quad (17)$$

with  $\pm \alpha_1, \pm \alpha_2$  being the roots of the characteristic equation of Lam SGT as

$$1 - \left( \frac{v^2 \rho^2}{2(1+v)} + \ell_0^2 \frac{(1-2v)^2}{(1+v)} + \ell_1^2 \frac{2(1+2v)^2}{5(1+v)} \right) \alpha^2 + \left( \ell_1^2 \frac{4v^2 \rho^2}{15(1+v)} + \ell_2^2 \frac{v^2 \rho^2}{8(1+v)} \right) \alpha^4 = 0 \quad (18)$$

and Aifantis SGT as

$$1 - \left( \frac{v^2 \rho^2}{2(1+v)} + \ell_s^2 \right) \alpha^2 + \left( \ell_s^2 \frac{v^2 \rho^2}{2(1+v)} \right) \alpha^4 = 0. \quad (19)$$

Lastly, integrating the differential condition of kinematic compatibility Eq. (2.1), the axial displacement field  $u$  can be detected in terms of the integration constant  $\Lambda_6$  as

$$u(x) = \int_0^x \varepsilon(\zeta) d\zeta + \Lambda_6. \quad (20)$$

Prescribing the standard kinematic and static boundary conditions (BC) Eq. (7.2) together with the new constitutive boundary conditions (CBC), Eqs. (11.2,3) of Lam SGT and Eqs. (13.2,3) of Aifantis SGT, the integration constants  $\Lambda_i$  ( $i = 1 \dots 6$ ) can be determined. The proposed solution method is variationally consistent providing exact elastic solutions by integrating differential equations of lower order when compared with those of literature. The proposed technique is simple and adequate also for solving a wide variety of structural problems.

Three case studies will be studied including a fixed-free nano-rod under a tensile axial force at the free end in addition to uniformly loaded nano-rods with fixed-fixed and fixed-free ends.

### 5.1 Tip-loaded nano-rod with fixed-free ends

For a strain gradient Bishop rod with fixed-free ends subjected to a tensile concentrated axial force  $\bar{N}$  at the free end, the classical BCs are well established to be

$$u(0) = 0, \quad N(L) = \bar{N}. \quad (21)$$

The non-dimensional axial displacement can be evaluated employing the proposed solution method while imposing the classical BCs and CBCs of Aifantis and Lam SGTs as

$$\bar{u}_{\text{Lam}}^{\text{SGT}}(\bar{x}) = \bar{u}_{\text{Aifantis}}^{\text{SGT}}(\bar{x}) = \bar{x} \quad (22)$$

which coincides with the results of the classical elastic model of slender rods. It can be inferred from Eq. (22) that the elastic axial response of a tip-loaded strain gradient nano-rod with fixed-free ends for both the modified and simplified strain gradient theories is not only independent of the characteristic parameter  $\lambda$  but also independent of the dimensionless gyration radius  $\bar{\rho}$ .

### 5.2 Uniformly loaded nano-rod with fixed-free ends

In case of a uniformly loaded strain gradient Bishop rod with fixed-free ends, the classical BCs are expressed by

$$u(0) = 0, \quad N(L) = 0. \quad (23)$$

The axial displacement of the nano-rod is detected employing the aforementioned solution method, prescribing the classical BCs and corresponding CBCs of Aifantis and Lam SGTs. It may be shown that the maximum value of the axial displacement field for both the modified and simplified strain gradient theories is given by

$$\bar{u}_{\text{Lam}}^{\text{SGT}}|_{\text{max}} = \bar{u}_{\text{Aifantis}}^{\text{SGT}}|_{\text{max}} = \frac{1}{2}. \quad (24)$$

The maximum axial deformation of the strain gradient Bishop rod at the free end, according to Aifantis and Lam SGTs, is coincident with the one obtained by the classical local elasticity model of slender rods. It is independent of both the characteristic parameter  $\lambda$  and non-dimensional gyration radius  $\bar{\rho}$ . The value of the axial displacement field at the mid-span of the rod is therefore examined for numerical illustrations.

### 5.3 Uniformly loaded nano-rod with fixed-fixed ends

When a strain gradient Bishop rod is subjected to the uniform axial load with fixed-fixed ends, the kinematic BCs are expressed as

$$u(0) = 0, \quad u(L) = 0. \quad (25)$$

In consequence of exploiting the proposed solution procedure while prescribing the classical BCs and corresponding CBCs of Aifantis and Lam SGTs, the axial displacement of the nano-rod can be determined.

### 5.4 Numerical results and discussion

Since the axial response of strain gradient elastic Bishop rods subjected to tensile axial tip-force, in accordance with both the modified and simplified gradient theories, is coincident with the axial response of classical elastic slender rods, it has been omitted from illustrations.

The dependency of the characteristic parameter  $\lambda$  on the non-dimensional maximum axial displacement corresponding to the modified and simplified strain gradient theories for uniformly loaded nano-rods with fixed-fixed and fixed-free ends is depicted in Figs. 1 and 2. Since the maximum axial deformation of uniformly loaded Bishop rods, associated with both Aifantis and Lam SGTs, coincides with the results of the classical elastic model of slender rods, the value of the axial displacement field at the mid-span of the rod is illustrated

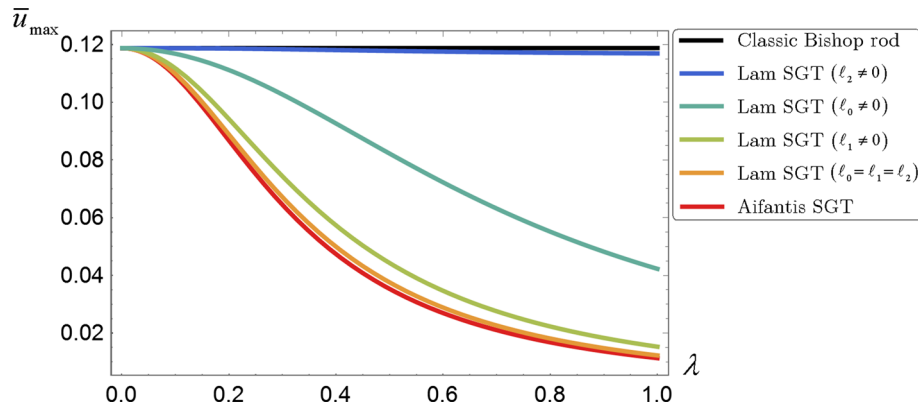


Fig. 1 Uniformly loaded nano-rod with fixed-fixed ends: effects of  $\lambda$  on  $\bar{u}_{\max}$  for  $\bar{\rho} = 0.5$

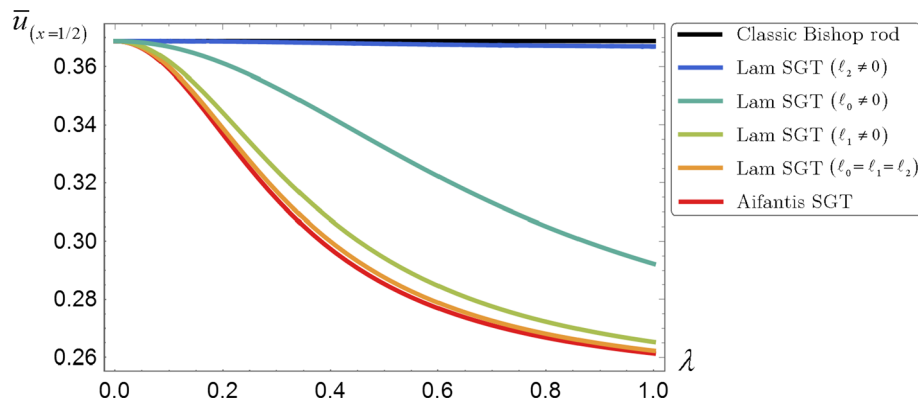


Fig. 2 Uniformly loaded nano-rod with fixed-free ends: effects of  $\lambda$  on  $\bar{u}_{(\bar{x}=1/2)}$  for  $\bar{\rho} = 0.5$

in Fig. 2. Also in the framework of Aifantis and Lam strain gradient theories, 3D plots of variations of the non-dimensional axial displacement  $\bar{u}$  versus the non-dimensional abscissa  $\bar{x}$  and characteristic parameter  $\lambda$  are shown in Figs. 3 and 4 for uniformly loaded nano-rods with fixed-fixed and fixed-free ends. The characteristic parameter  $\lambda$  is assumed to range in the interval  $]0, 1[$ , and the non-dimensional gyration radius is assumed to be  $\bar{\rho} = 0.5$ . To examine the effects of the characteristic parameter  $\lambda$  on axial responses of Bishop nano-rods, the Poisson ratio  $\nu = 1/4$  is considered in all illustrations.

It is inferred from Figs. 1 through 4 that the nano-rod axial displacement field will decrease as the characteristic parameter  $\lambda$  increases, and therefore, both modified and simplified strain gradient elasticity theories exhibit a stiffening behavior in terms of the characteristic parameter  $\lambda$  for a given value of  $\bar{\rho}$ . While the gradient parameter  $\ell_2$  characterizing the rotation gradient exhibits the less stiffening effect, the gradient parameter  $\ell_1$  reflecting the stretch gradient shows the dominant stiffening effect of gradient parameters in the Lam SGT.

As expected, the modified strain gradient theory with equal gradient parameters  $\ell_0 = \ell_1 = \ell_2$  has the maximum decreasing effect on the axial displacement field in comparison with individual gradient parameters of Lam SGT. Furthermore, the stiffening effect of the characteristic parameter in the framework of Aifantis SGT is more noticeable in comparison with the Lam SGT with  $\ell_0 = \ell_1 = \ell_2$ . For vanishing non-dimensional characteristic parameter  $\lambda \rightarrow 0^+$ , the size-dependent elastostatic response of a strain gradient Bishop nano-rod is also coincident with the one of a classical Bishop elastic thick rod. Numerical values of the non-dimensional axial displacement  $\bar{u}$  at the mid-span of uniformly loaded nano-rods with fixed-fixed and fixed-free ends for each of the described conditions in the Lam strain gradient theory as well as the Aifantis strain gradient theory are, respectively, collected in Tables 1 and 2 in terms of the characteristic parameter  $\lambda$ .

Variations of the non-dimensional axial displacement at the structural mid-span, associated with the modified and simplified strain gradient theories, for uniformly loaded nano-rods with fixed-fixed and fixed-free ends in terms of gyration radius  $\bar{\rho}$  are given in Figs. 5 and 6. Furthermore, 3D plots exhibiting the effects of the gyration radius  $\bar{\rho}$  on the axial deformation  $\bar{u}$  versus the axial abscissa  $\bar{x}$  for uniformly loaded nano-rods with fixed-fixed and fixed-free ends are, respectively, illustrated in Figs. 7 and 8 for both Aifantis and Lam



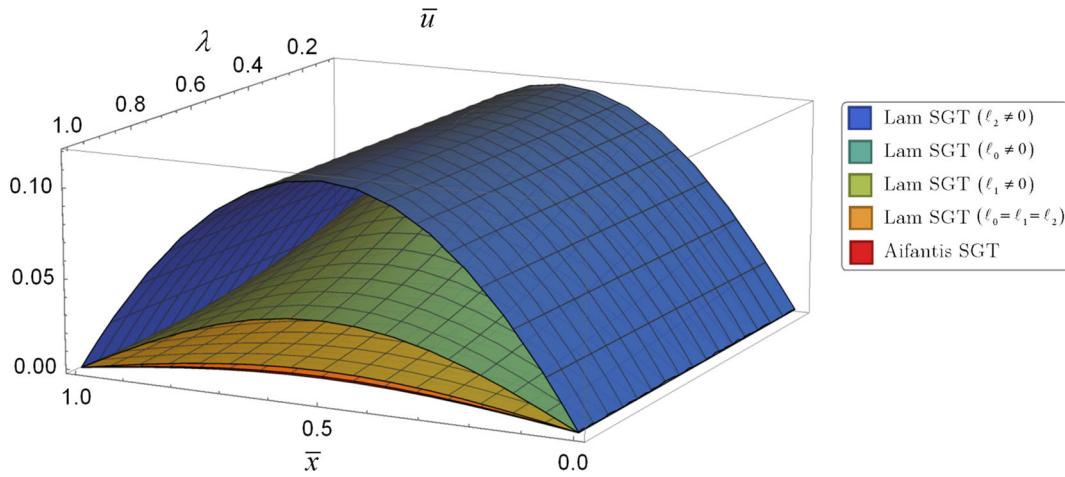


**Fig. 3** Uniformly loaded nano-rod with fixed-fixed ends:  $\bar{u}$  versus  $\bar{x}$  and  $\lambda$  for  $\bar{\rho} = 0.5$

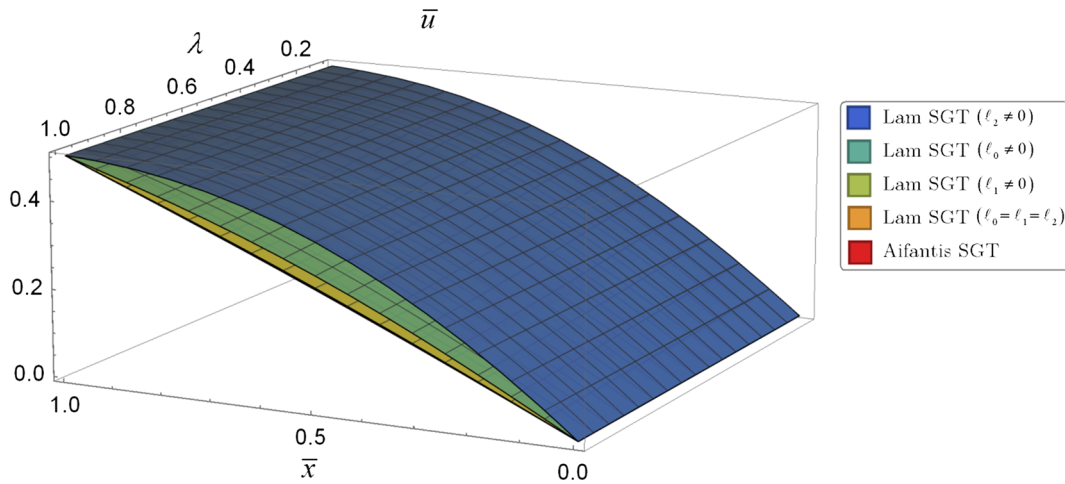


**Fig. 4** Uniformly loaded nano-rod with fixed-free ends:  $\bar{u}$  versus  $\bar{x}$  and  $\lambda$  for  $\bar{\rho} = 0.5$

SGTs. While the gyration radius is ranging in the interval  $]0.1, 0.5[$ , the characteristic parameter  $\lambda$  is assumed to be  $\lambda = 0.2$ . Once more, the Poisson ratio is assumed as  $\nu = 1/4$  in all illustrative results.

It is deduced from Figs. 5 through 8 that the axial displacement field for both Aifantis and Lam SGTs reveals a stiffening behavior in terms of the gyration radius. A larger  $\bar{\rho}$  involves a smaller displacement  $\bar{u}$  for a given value of  $\lambda$ . The numerical values of the maximum axial displacement  $\bar{u}_{\max}$  of a uniformly loaded nano-rod with fixed-fixed ends for modified and simplified SGTs are reported in Table 3 in terms of the gyration radius  $\bar{\rho}$ .

In case of uniformly loaded nano-rods with fixed-free ends, since the maximum axial deformation of strain gradient Bishop rods at the free end is independent of both the characteristic parameter and gyration radius, numerical values of the axial displacement at the structural mid-span in terms of the gyration radius  $\bar{\rho}$  are given in Table 4 for both Aifantis and Lam SGTs.

### 6 Concluding remarks

The major outcomes of the present study may be summarized as follows.

- The contributions in literature on Bishop’s rod model, based on strain gradient elasticity theory, suffer from the lack of suitable prescription of constitutive boundary conditions. This point has been addressed for both Lam and Aifantis models by making recourse to a consistent variational approach with suitably selected test fields.



**Table 1** Uniformly loaded Bishop nano-rod with fixed-fixed ends:  $\bar{u}_{\max}$  versus  $\lambda$  and  $\bar{\rho} = 0.5$

$\lambda$	$\bar{u}_{\max}$				
	Lam SGT $\ell_0 \neq 0$	Lam SGT $\ell_1 \neq 0$	Lam SGT $\ell_2 \neq 0$	Lam SGT $\ell_0 = \ell_1 = \ell_2$	Aifantis SGT
0+	0.118772	0.118772	0.118772	0.118772	0.118772
0.1	0.116817	0.111781	0.118747	0.109898	0.109126
0.2	0.111182	0.094201	0.118635	0.088847	0.086771
0.3	0.102703	0.074333	0.1184	0.067097	0.064459
0.4	0.092649	0.057326	0.118106	0.04993	0.047363
0.5	0.082215	0.044283	0.117818	0.037562	0.035313
0.6	0.072233	0.034643	0.117566	0.028831	0.026935
0.7	0.063151	0.027554	0.117355	0.022618	0.021036
0.8	0.055143	0.02229	0.117184	0.018113	0.016793
0.9	0.048209	0.018323	0.117045	0.014777	0.013668
1.0	0.042267	0.015283	0.116933	0.012255	0.011315

**Table 2** Uniformly loaded Bishop nano-rod with fixed-free ends:  $\bar{u}_{x=1/2}$  versus  $\lambda$  and  $\bar{\rho} = 0.5$

$\lambda$	$\bar{u}_{x=1/2}$				
	Lam SGT $\ell_0 \neq 0$	Lam SGT $\ell_1 \neq 0$	Lam SGT $\ell_2 \neq 0$	Lam SGT $\ell_0 = \ell_1 = \ell_2$	Aifantis SGT
0+	0.368772	0.368772	0.368772	0.368772	0.368772
0.1	0.366817	0.361781	0.368747	0.359898	0.359126
0.2	0.361182	0.344201	0.368635	0.338847	0.336771
0.3	0.352703	0.324333	0.3684	0.317097	0.314459
0.4	0.342649	0.307326	0.368106	0.299929	0.297363
0.5	0.332215	0.294283	0.367818	0.287562	0.285313
0.6	0.322233	0.284643	0.367566	0.278831	0.276935
0.7	0.313151	0.277554	0.367355	0.272617	0.271036
0.8	0.305143	0.27229	0.367184	0.268113	0.266793
0.9	0.298209	0.268323	0.367045	0.264777	0.263668
1.0	0.292267	0.265282	0.366933	0.262255	0.261314

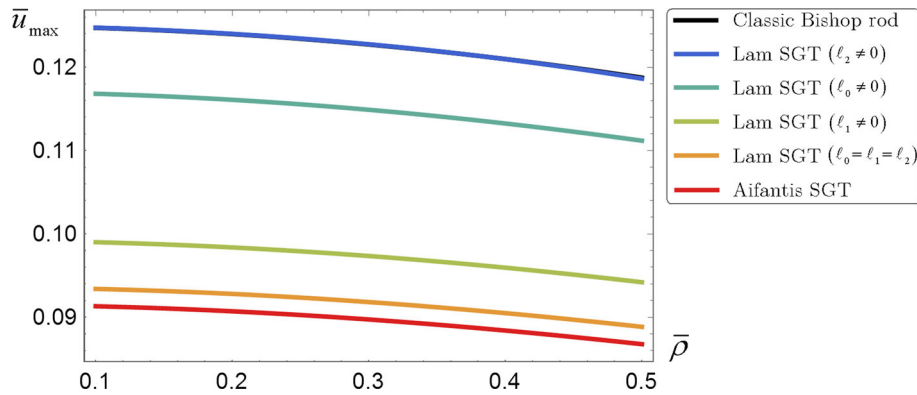


**Fig. 5** Uniformly loaded nano-rod with fixed-fixed ends: effects of  $\bar{\rho}$  on  $\bar{u}_{\max}$  for  $\lambda = 0.2$

- The developed strain gradient formulations have been shown to be well posed and therefore are able to describe the size-dependent static behavior of Bishop nano-rods.
- The proposed solution procedure, being variationally consistent, has the advantage of providing analytical solutions by integrating differential equations of lower order.
- Elastostatic axial responses of Bishop nano-rods made of Aifantis and Lam strain gradient materials exhibit a stiffening behavior for smaller and smaller structures.
- The gradient parameters  $\ell_2$  and  $\ell_1$ , respectively, characterizing rotation and stretch gradients in Lam SGT, demonstrate the minimum and maximum stiffening effects of the gradient parameters in the modified strain gradient theory.
- The modified strain gradient theory with equal scale parameters  $\ell_0 = \ell_1 = \ell_2$  has the maximum decreasing effect on the axial displacement field in comparison with individual gradient parameters of Lam SGT.

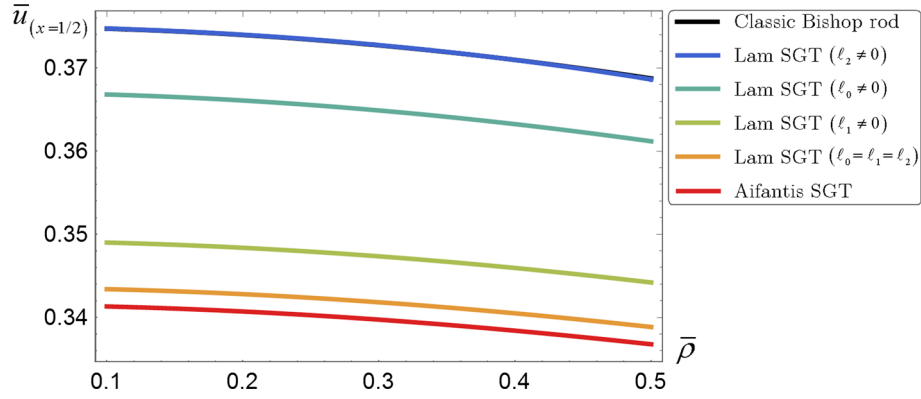


Fig. 6 Uniformly loaded nano-rod with fixed-free ends: effects of  $\bar{\rho}$  on  $\bar{u}_{(\bar{x}=1/2)}$  for  $\lambda = 0.2$

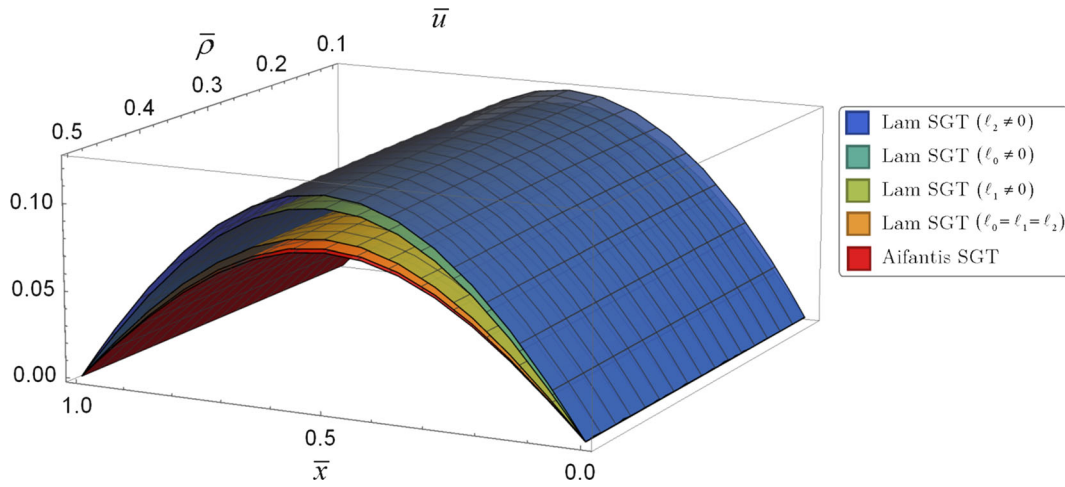


Fig. 7 Uniformly loaded nano-rod with fixed-fixed ends:  $\bar{u}$  versus  $\bar{x}$  and  $\bar{\rho}$  for  $\lambda = 0.2$

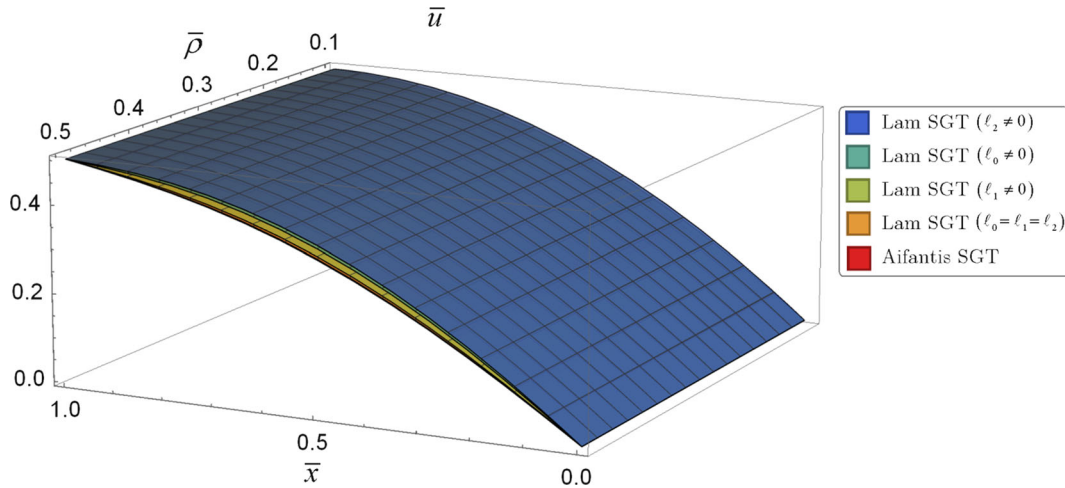


Fig. 8 Uniformly loaded nano-rod with fixed-free ends:  $\bar{u}$  versus  $\bar{x}$  and  $\bar{\rho}$  for  $\lambda = 0.2$

**Table 3** Uniformly loaded Bishop nano-rod with fixed-fixed ends:  $\bar{u}_{\max}$  versus  $\bar{\rho}$  and  $\lambda = 0.2$ 

$\bar{\rho}$	$\bar{u}_{\max}$				
	Lam SGT $\ell_0 \neq 0$	Lam SGT $\ell_1 \neq 0$	Lam SGT $\ell_2 \neq 0$	Lam SGT $\ell_0 = \ell_1 = \ell_2$	Aifantis SGT
0.1	0.116817	0.099006	0.12475	0.093398	0.091317
0.2	0.116093	0.098377	0.124003	0.092798	0.090712
0.3	0.114897	0.09735	0.122753	0.09182	0.089732
0.4	0.11325	0.095947	0.120966	0.090492	0.088405
0.5	0.111182	0.094201	0.118635	0.088847	0.086771

**Table 4** Uniformly loaded Bishop nano-rod with fixed-free ends:  $\bar{u}_{x=1/2}$  versus  $\bar{\rho}$  and  $\lambda = 0.2$ 

$\bar{\rho}$	$\bar{u}_{x=1/2}$				
	Lam SGT $\ell_0 \neq 0$	Lam SGT $\ell_1 \neq 0$	Lam SGT $\ell_2 \neq 0$	Lam SGT $\ell_0 = \ell_1 = \ell_2$	Aifantis SGT
0.1	0.366817	0.349006	0.37475	0.343398	0.341317
0.2	0.366093	0.348377	0.374003	0.342798	0.340712
0.3	0.364897	0.34735	0.372753	0.34182	0.339732
0.4	0.36325	0.345947	0.370966	0.340492	0.338405
0.5	0.361182	0.344201	0.368635	0.338847	0.336771

- The stiffening effect of the characteristic parameter according to the simplified strain gradient theory is more noticeable in comparison with the modified strain gradient theory with equal gradient parameters.
- Both the modified and simplified strain gradient elastic models of the Bishop rod lead to the results of the classic Bishop rod local model for vanishing scale parameters.
- As physically expected, the gyration radius has the effect of decreasing the axial deformation of the Bishop rod in both Aifantis and Lam strain gradient elasticity theories.
- In both modified and simplified strain gradient models, the maximum axial deformation of uniformly loaded nano-rods with fixed-free ends is independent of scale parameters and gyration radius and coincides with the classical elastic local deformation of slender rods.
- In the frameworks of Aifantis and Lam SGTs, the elastic axial response of tip-loaded nano-rods with fixed-free ends is independent of characteristic parameters and gyration radius, being coincident with the one of classical slender rods.
- The contributed results provide a useful guide for the design of small sensors and actuators for current nanotechnological applications.

## References

1. Acierno, S., Barretta, R., Luciano, R., Marotti de Sciarra, F., Russo, P.: Experimental evaluations and modeling of the tensile behavior of polypropylene/single-walled carbon nanotubes fibers. *Compos. Struct.* **174**, 12–18 (2017). <https://doi.org/10.1016/j.compstruct.2017.04.049>
2. Barretta, R., Brcic, M., Canadija, M., Luciano, R., Marotti de Sciarra, F.: Application of gradient elasticity to armchair carbon nanotubes: size effects and constitutive parameters assessment. *Eur. J. Mech. A Solids* **65**, 1–13 (2017). <https://doi.org/10.1016/j.euromechsol.2017.03.002>
3. Romano, G., Barretta, R.: Nonlocal elasticity in nanobeams: the stress-driven integral model. *Int. J. Eng. Sci.* **115**, 14–27 (2017). <https://doi.org/10.1016/j.ijengsci.2017.03.002>
4. Faghidian, S.A.: Reissner stationary variational principle for nonlocal strain gradient theory of elasticity. *Eur. J. Mech. A Solids* **70**, 115–126 (2018). <https://doi.org/10.1016/j.euromechsol.2018.02.009>
5. Faghidian, S.A.: On non-linear flexure of beams based on non-local elasticity theory. *Int. J. Eng. Sci.* **124**, 49–63 (2018). <https://doi.org/10.1016/j.ijengsci.2017.12.002>
6. Faghidian, S.A.: Integro-differential nonlocal theory of elasticity. *Int. J. Eng. Sci.* **129**, 96–110 (2018). <https://doi.org/10.1016/j.ijengsci.2018.04.007>
7. Barretta, R., Marotti de Sciarra, F.: Constitutive boundary conditions for nonlocal strain gradient elastic nano-beams. *Int. J. Eng. Sci.* **130**, 187–198 (2018). <https://doi.org/10.1016/j.ijengsci.2018.05.009>
8. Zhang, L., Guo, J., Xing, Y.: Nonlocal analytical solution of functionally graded multilayered one-dimensional hexagonal piezoelectric quasicrystal nanoplates. *Acta Mech.* (2019). <https://doi.org/10.1007/s00707-018-2344-7>
9. Attia, M.A., Mohamed, S.A.: Coupling effect of surface energy and dispersion forces on nonlinear size-dependent pull-in instability of functionally graded micro-/nanoswitches. *Acta Mech.* (2019). <https://doi.org/10.1007/s00707-018-2345-6>

10. Gharahi, A., Schiavone, P.: Edge dislocation with surface flexural resistance in micropolar materials. *Acta Mech.* (2019). <https://doi.org/10.1007/s00707-018-2338-5>
11. Genoese, A., Genoese, A., Salerno, G.: On the nanoscale behaviour of single-wall C, BN and SiC nanotubes. *Acta Mech.* (2019). <https://doi.org/10.1007/s00707-018-2336-7>
12. Bunoiu, R., Gaudiello, A., Leopardi, A.: Asymptotic analysis of a Bingham fluid in a thin T-like shaped structure. *J. Math. Pures Appl.* **123**, 148–166 (2019). <https://doi.org/10.1016/j.matpur.2018.01.001>
13. Zhang, Y.P., Challamel, N., Wang, C.M., Zhang, H.: Comparison of nano-plate bending behaviour by Eringen nonlocal plate, Hencky bar-net and continualised nonlocal plate models. *Acta Mech.* (2018). <https://doi.org/10.1007/s00707-018-2326-9>
14. Romano, G., Barretta, R., Diaco, M.: Iterative methods for nonlocal elasticity problems. *Continuum Mech. Thermodyn.* **31**, 669–689 (2019). <https://doi.org/10.1007/s00161-018-0717-8>
15. Rashahmadi, S., Meguid, S.A.: Modeling size-dependent thermoelastic energy dissipation of graphene nanoresonators using nonlocal elasticity theory. *Acta Mech.* (2018). <https://doi.org/10.1007/s00707-018-2281-5>
16. Bahreman, M., Darijani, H., Bahrani Fard, A.: The size-dependent analysis of microplates via a newly developed shear deformation theory. *Acta Mech.* (2018). <https://doi.org/10.1007/s00707-018-2260-x>
17. Zhang, G.Y., Gao, X.L.: A non-classical Kirchhoff rod model based on the modified couple stress theory. *Acta Mech.* (2018). <https://doi.org/10.1007/s00707-018-2279-z>
18. Lembo, M.: Infinitesimal deformations and stability of rods made of nonlocal elastic materials. *Acta Mech.* (2018). <https://doi.org/10.1007/s00707-018-2315-z>
19. Radgolchin, M., Moeenfard, H.: Size-dependent nonlinear vibration analysis of shear deformable microarches using strain gradient theory. *Acta Mech.* **229**, 3025–3049 (2018). <https://doi.org/10.1007/s00707-018-2142-2>
20. Sidhardh, S., Ray, M.C.: Element-free Galerkin model of nano-beams considering strain gradient elasticity. *Acta Mech.* **229**, 2765–2786 (2018). <https://doi.org/10.1007/s00707-018-2139-x>
21. Chen, H., Qi, C., Efremidis, G., Dorogov, M., Aifantis, E.C.: Gradient elasticity and size effect for the borehole problem. *Acta Mech.* **229**, 3305–3318 (2018). <https://doi.org/10.1007/s00707-018-2109-3>
22. Gaudiello, A., Panasenko, G., Piatnitski, A.: Asymptotic analysis and domain decomposition for a biharmonic problem in a thin multi-structure. *Commun. Contemp. Math.* **18**, 1550057 (2016). <https://doi.org/10.1142/S0219199715500571>
23. Koutsoumaris, C.C., Eptameris, K.G.: A research into bi-Helmholtz type of nonlocal elasticity and a direct approach to Eringen's nonlocal integral model in a finite body. *Acta Mech.* **229**, 3629–3649 (2018). <https://doi.org/10.1007/s00707-018-2180-9>
24. Sidhardh, S., Ray, M.C.: Inclusion problem for a generalized strain gradient elastic continuum. *Acta Mech.* **229**, 3813–3831 (2018). <https://doi.org/10.1007/s00707-018-2199-y>
25. Fan, H., Xu, L.: Love wave in a classical linear elastic half-space covered by a surface layer described by the couple stress theory. *Acta Mech.* **229**, 5121–5132 (2018). <https://doi.org/10.1007/s00707-018-2293-1>
26. Polyanskiy, A.M., Polyanskiy, V.A., Belyaev, A.K., Yakovlev, Y.A.: Relation of elastic properties, yield stress and ultimate strength of polycrystalline metals to their melting and evaporation parameters with account for nano and micro structure. *Acta Mech.* **229**, 4863–4873 (2018). <https://doi.org/10.1007/s00707-018-2262-8>
27. Cajić, M., Lazarević, M., Karličić, D., Sun, H., Liu, X.: Fractional-order model for the vibration of a nanobeam influenced by an axial magnetic field and attached nanoparticles. *Acta Mech.* **229**, 4791–4815 (2018). <https://doi.org/10.1007/s00707-018-2263-7>
28. Gaudiello, A., Kolpakov, A.G.: Influence of non degenerated joint on the global and local behavior of joined rods. *Int. J. Eng. Sci.* **49**, 295–309 (2011). <https://doi.org/10.1016/j.ijengsci.2010.11.002>
29. Guo, J., Li, X.: Surface effects on an electrically permeable elliptical nano-hole or nano-crack in piezoelectric materials under anti-plane shear. *Acta Mech.* **229**, 4251–4266 (2018). <https://doi.org/10.1007/s00707-018-2232-1>
30. Apuzzo, A., Barretta, R., Faghidian, S.A., Luciano, R., Marotti de Sciarra, F.: Free vibrations of elastic beams by modified nonlocal strain gradient theory. *Int. J. Eng. Sci.* **133**, 99–108 (2018). <https://doi.org/10.1016/j.ijengsci.2018.09.002>
31. Apuzzo, A., Barretta, R., Faghidian, S.A., Luciano, R., Marotti de Sciarra, F.: Nonlocal strain gradient exact solutions for functionally graded inflected nano-beams. *Compos. Part B* **164**, 667–674 (2019). <https://doi.org/10.1016/j.compositesb.2018.12.112>
32. Civalek, Ö., Akgöz, B., Deliktaş, B.: Axial vibration of strain gradient micro-rods. In: Voyiadjis, G. (ed.) *Handbook of Nonlocal Continuum Mechanics for Materials and Structures*, pp. 1141–1155. Springer, Cham (2019). [https://doi.org/10.1007/978-3-319-58729-5\\_7](https://doi.org/10.1007/978-3-319-58729-5_7)
33. Numanoğlu, H.M., Akgöz, B., Civalek, Ö.: On dynamic analysis of nanorods. *Int. J. Eng. Sci.* **130**, 33–50 (2018). <https://doi.org/10.1016/j.ijengsci.2018.05.001>
34. Akgöz, B., Civalek, Ö.: Longitudinal vibration analysis for microbars based on strain gradient elasticity theory. *J. Vib. Control* **20**, 606–616 (2014). <https://doi.org/10.1177/1077546312463752>
35. Akgöz, B., Civalek, Ö.: Longitudinal vibration analysis of strain gradient bars made of functionally graded materials (FGM). *Compos. Part B* **55**, 263–268 (2013). <https://doi.org/10.1016/j.compositesb.2013.06.035>
36. Demir, Ç., Civalek, Ö.: Torsional and longitudinal frequency and wave response of microtubules based on the nonlocal continuum and nonlocal discrete models. *Appl. Math. Model.* **37**, 9355–9367 (2013). <https://doi.org/10.1016/j.apm.2013.04.050>
37. Aifantis, E.C.: Internal length gradient (ILG) material mechanics across scales and disciplines. *Adv. Appl. Mech.* **49**, 1–110 (2016). <https://doi.org/10.1016/bs.aams.2016.08.001>
38. Farajpour, A., Ghayesh, M.H., Farokhi, H.: A review on the mechanics of nanostructures. *Int. J. Eng. Sci.* **133**, 231–263 (2018). <https://doi.org/10.1016/j.ijengsci.2018.09.006>
39. Ghayesh, M.H., Farajpour, A.: A review on the mechanics of functionally graded nanoscale and microscale structures. *Int. J. Eng. Sci.* **137**, 8–36 (2019). <https://doi.org/10.1016/j.ijengsci.2018.12.001>
40. Romano, G., Barretta, R., Diaco, M., Marotti de Sciarra, F.: Constitutive boundary conditions and paradoxes in nonlocal elastic nano-beams. *Int. J. Mech. Sci.* **121**, 151–156 (2017). <https://doi.org/10.1016/j.ijmecsci.2016.10.036>

41. Romano, G., Barretta, R., Diaco, M.: On nonlocal integral models for elastic nanobeams. *Int. J. Mech. Sci.* **131**, 490–499 (2017). <https://doi.org/10.1016/j.ijmecsci.2017.07.013>
42. Romano, G., Luciano, R., Barretta, R., Diaco, M.: Nonlocal integral elasticity in nanostructures, mixtures, boundary effects and limit behaviours. *Continuum Mech. Thermodyn.* **30**, 641–655 (2018). <https://doi.org/10.1007/s00161-018-0631-0>
43. Romano, G., Barretta, R.: Stress-driven versus strain-driven nonlocal integral model for elastic nano-beams. *Compos. Part B* **114**, 184–188 (2017). <https://doi.org/10.1016/j.compositesb.2017.01.008>
44. Apuzzo, A., Barretta, R., Luciano, R., de Sciarra, F.M., Penna, R.: Free vibrations of Bernoulli–Euler nano-beams by the stress-driven nonlocal integral model. *Compos. Part B* **123**, 105–111 (2017). <https://doi.org/10.1016/j.compositesb.2017.03.057>
45. Barretta, R., Canadija, M., Feo, L., Luciano, R., Marotti de Sciarra, F., Penna, R.: Exact solutions of inflected functionally graded nano-beams in integral elasticity. *Compos. Part B* **142**, 273–286 (2018). <https://doi.org/10.1016/j.compositesb.2017.12.022>
46. Barretta, R., Faghidian, S.A., Luciano, R., Medaglia, C.M., Penna, R.: Free vibrations of FG elastic Timoshenko nano-beams by strain gradient and stress driven nonlocal models. *Compos. Part B* **154**, 20–32 (2018). <https://doi.org/10.1016/j.compositesb.2018.07.036>
47. Barretta, R., Canadija, M., Luciano, R., Marotti de Sciarra, F.: Stress-driven modeling of nonlocal thermoelastic behavior of nanobeams. *Int. J. Eng. Sci.* **126**, 53–67 (2018). <https://doi.org/10.1016/j.ijengsci.2018.02.012>
48. Barretta, R., Diaco, M., Feo, L., Luciano, R., Marotti de Sciarra, F., Penna, R.: Stress-driven integral elastic theory for torsion of nano-beams. *Mech. Res. Commun.* **87**, 35–41 (2018). <https://doi.org/10.1016/j.mechrescom.2017.11.004>
49. Barretta, R., Luciano, R., Marotti de Sciarra, F., Ruta, G.: Stress-driven nonlocal integral model for Timoshenko elastic nano-beams. *Eur. J. Mech. A Solids* **72**, 275–286 (2018). <https://doi.org/10.1016/j.euromechsol.2018.04.012>
50. Barretta, R., Fazelzadeh, S.A., Feo, L., Ghavanloo, E., Luciano, R.: Nonlocal inflected nano-beams: a stress-driven approach of bi-Helmholtz type. *Compos. Struct.* **200**, 239–245 (2018). <https://doi.org/10.1016/j.compstruct.2018.04.072>
51. Mahmoudpour, E., Hosseini-Hashemi, S., Faghidian, S.A.: Non-linear vibration analysis of FG nano-beams resting on elastic foundation in thermal environment using stress-driven nonlocal integral model. *Appl. Math. Model.* **57**, 302–315 (2018). <https://doi.org/10.1016/j.apm.2018.01.021>
52. Barretta, R., Faghidian, S.A., Luciano, R.: Longitudinal vibrations of nano-rods by stress-driven integral elasticity. *Mech. Adv. Mater. Struct.* (2019). <https://doi.org/10.1080/15376494.2018.1432806>
53. Barretta, R., Caporale, A., Faghidian, S.A., Luciano, R., Marotti de Sciarra, F., Medaglia, C.M.: A stress-driven local-nonlocal mixture model for Timoshenko nano-beams. *Compos. Part B* **164**, 590–598 (2019). <https://doi.org/10.1016/j.compositesb.2019.01.012>
54. Barretta, R., Fabbrocino, F., Luciano, R., Marotti de Sciarra, F.: Closed-form solutions in stress-driven two-phase integral elasticity for bending of functionally graded nano-beams. *Physica E* **97**, 13–30 (2018). <https://doi.org/10.1016/j.physe.2017.09.026>
55. Barretta, R., Faghidian, S.A., Luciano, R., Medaglia, C.M., Penna, R.: Stress-driven two-phase integral elasticity for torsion of nano-beams. *Compos. Part B* **145**, 62–69 (2018). <https://doi.org/10.1016/j.compositesb.2018.02.020>
56. Apuzzo, A., Barretta, R., Fabbrocino, F., Faghidian, S.A., Luciano, R., Marotti de Sciarra, F.: Axial and torsional free vibrations of elastic nano-beams by stress-driven two-phase elasticity. *J. Appl. Comput. Mech.* **5**, 402–413 (2019). <https://doi.org/10.22055/jacm.2018.26552.1338>
57. Barretta, R., Faghidian, S.A., Marotti de Sciarra, F.: Stress-driven nonlocal integral elasticity for axisymmetric nano-plates. *Int. J. Eng. Sci.* **136**, 38–52 (2019). <https://doi.org/10.1016/j.ijengsci.2019.01.003>
58. Barretta, R., Fabbrocino, F., Luciano, R., Marotti de Sciarra, F., Ruta, G.: Buckling loads of nano-beams in stress-driven nonlocal elasticity. *Mech. Adv. Mater. Struct.* (2019). <https://doi.org/10.1080/15376494.2018.1501523>
59. Mindlin, R.D.: Second gradient of strain and surface-tension in linear elasticity. *Int. J. Solids Struct.* **1**, 417–438 (1965). [https://doi.org/10.1016/0020-7683\(65\)90006-5](https://doi.org/10.1016/0020-7683(65)90006-5)
60. Aifantis, E.C.: On the role of gradients in the localization of deformation and fracture. *Int. J. Eng. Sci.* **3**, 1279–1299 (1992). [https://doi.org/10.1016/0020-7225\(92\)90141-3](https://doi.org/10.1016/0020-7225(92)90141-3)
61. Lam, D.C.C., Yang, F., Chong, A.C.M., Wang, J., Tong, P.: Experiments and theory in strain gradient elasticity. *J. Mech. Phys. Solids* **51**, 1477–1508 (2003). [https://doi.org/10.1016/S0022-5096\(03\)00053-X](https://doi.org/10.1016/S0022-5096(03)00053-X)
62. Kong, S., Zhou, S., Nie, Z., Wang, K.: Static and dynamic analysis of micro beams based on strain gradient elasticity theory. *Int. J. Eng. Sci.* **47**, 487–498 (2009). <https://doi.org/10.1016/j.ijengsci.2008.08.008>
63. Askes, H., Aifantis, E.C.: Gradient elasticity in statics and dynamics: an overview of formulations, length scale identification procedures, finite element implementations and new results. *Int. J. Solids Struct.* **48**, 1962–1990 (2011). <https://doi.org/10.1016/j.ijsolstr.2011.03.006>
64. Zhou, S., Li, A., Wang, B.: A reformulation of constitutive relations in the strain gradient elasticity theory for isotropic materials. *Int. J. Solids Struct.* **80**, 28–37 (2016). <https://doi.org/10.1016/j.ijsolstr.2015.10.018>
65. Zhao, B., Liu, T., Chen, J., Peng, X., Song, Z.: A new Bernoulli–Euler beam model based on modified gradient elasticity. *Arch. Appl. Mech.* (2018). <https://doi.org/10.1007/s00419-018-1464-9>
66. Polizzotto, C.: A hierarchy of simplified constitutive models within isotropic strain gradient elasticity. *Eur. J. Mech. A Solids* **61**, 92–109 (2017). <https://doi.org/10.1016/j.euromechsol.2016.09.006>
67. Polizzotto, C.: Anisotropy in strain gradient elasticity: simplified models with different forms of internal length and moduli tensors. *Eur. J. Mech. A Solids* **71**, 51–63 (2018). <https://doi.org/10.1016/j.euromechsol.2018.03.006>
68. Han, J.-B., Hong, S.-Y., Song, J.-H., Kwon, H.-W.: Vibrational energy flow models for the Rayleigh–Love and Rayleigh–Bishop rods. *J. Sound Vib.* **333**, 520–540 (2014). <https://doi.org/10.1016/j.jsv.2013.08.027>
69. Mei, C.: Comparison of the four rod theories of longitudinally vibrating rods. *J. Vib. Control.* **21**, 1639–1656 (2015). <https://doi.org/10.1177/1077546313494216>
70. Aydogdu, M.: Longitudinal wave propagation in nanorods using a general nonlocal unimodal rod theory and calibration of nonlocal parameter with lattice dynamics. *Int. J. Eng. Sci.* **56**, 17–28 (2012). <https://doi.org/10.1016/j.ijengsci.2012.02.004>



71. Ecsedi, I., Baksa, A.: Free axial vibration of nanorods with elastic medium interaction based on nonlocal elasticity and Rayleigh model. *Mech. Res. Commun.* **86**, 1–4 (2017). <https://doi.org/10.1016/j.mechrescom.2017.10.003>
72. Li, X.-F., Tang, G.-J., Shen, Z.-B., Lee, K.Y.: Size-dependent resonance frequencies of longitudinal vibration of a nonlocal Love nanobar with a tip nanoparticle. *Math. Mech. Solids* **22**, 1529–1542 (2017). <https://doi.org/10.1177/1081286516640597>
73. Li, X.-F., Shen, Z.-B., Lee, K.Y.: Axial wave propagation and vibration of nonlocal nanorods with radial deformation and inertia. *ZAMM J. Appl. Math. Mech.* **97**, 602–616 (2017). <https://doi.org/10.1002/zamm.201500186>
74. Liu, H., Liu, H., Yang, J.: Longitudinal waves in carbon nanotubes in the presence of transverse magnetic field and elastic medium. *Physica E* **93**, 153–159 (2017). <https://doi.org/10.1016/j.physe.2017.05.022>
75. Nazemnezhad, R., Kamali, K.: An analytical study on the size dependent longitudinal vibration analysis of thick nanorods. *Mater. Res. Express* **5**, 075016 (2018). <https://doi.org/10.1088/2053-1591/aac16e>
76. Nazemnezhad, R., Kamali, K.: Free axial vibration analysis of axially functionally graded thick nanorods using nonlocal Bishop's theory. *Steel Compos. Struct.* **28**, 749–758 (2018). <https://doi.org/10.12989/scs.2018.28.6.749>
77. Karličić, D.Z., Ayed, A., Flaieih, E.: Nonlocal axial vibration of the multiple Bishop nanorod system. *Math. Mech. Solids* (2018). <https://doi.org/10.1177/1081286518766577>
78. Güven, U.: Love–Bishop rod solution based on strain gradient elasticity theory. *C. R. Mec.* **342**, 8–16 (2014). <https://doi.org/10.1016/j.crme.2013.10.011>
79. Güven, U.: The investigation of the nonlocal longitudinal stress waves with modified couple stress theory. *Acta Mech.* **221**, 321–325 (2011). <https://doi.org/10.1007/s00707-011-0500-4>
80. Arefi, M., Zenkour, A.M.: Employing the coupled stress components and surface elasticity for nonlocal solution of wave propagation of a functionally graded piezoelectric Love nanorod model. *J. Intell. Mater. Syst. Struct.* **28**, 2403–2413 (2017). <https://doi.org/10.1177/1045389X17689930>
81. Güven, U.: A more general investigation for the longitudinal stress waves in microrods with initial stress. *Acta Mech.* **223**, 2065–2074 (2012). <https://doi.org/10.1007/s00707-012-0682-4>
82. Güven, U.: A generalized nonlocal elasticity solution for the propagation of longitudinal stress waves in bars. *Eur. J. Mech. A Solids* **45**, 75–79 (2014). <https://doi.org/10.1016/j.euromechsol.2013.11.014>
83. Güven, U.: General investigation for longitudinal wave propagation under magnetic field effect via nonlocal elasticity. *Appl. Math. Mech. Engl. Ed.* **36**, 1305–1318 (2015). <https://doi.org/10.1007/s10483-015-1985-9>
84. Arefi, M.: Surface effect and non-local elasticity in wave propagation of functionally graded piezoelectric nano-rod excited to applied voltage. *Appl. Math. Mech. Engl. Ed.* **37**, 289–302 (2016). <https://doi.org/10.1007/s10483-016-2039-6>
85. Arefi, M.: Analysis of wave in a functionally graded magneto-electro-elastic nano-rod using nonlocal elasticity model subjected to electric and magnetic potentials. *Acta Mech.* **227**, 2529–2542 (2016). <https://doi.org/10.1007/s00707-016-1584-7>
86. Rao, S.S.: *Vibration of Continuous Systems*. Wiley, Hoboken (2007)